Video Article

Preparation of Liquid-exfoliated Transition Metal Dichalcogenide Nanosheets with Controlled Size and Thickness: A State of the Art Protocol

Claudia Backes[1], Damien Hanlon[2], Beata M. Szydlowska[2], Andrew Harvey[2], Ronan J. Smith[2], Thomas M. Higgins[1], Jonathan N. Coleman[2]

[1]Chair of Applied Physical Chemistry, Ruprecht-Karls University Heidelberg

[2]School of Physics and CRANN, Trinity College Dublin

Correspondence to: Claudia Backes at backes@uni-heidelberg.de

URL: https://www.jove.com/video/54806
DOI: doi:10.3791/54806

Keywords: Engineering, Issue 118, layered materials, transition metal dichalcogenides, liquid exfoliation, size selection, centrifugation, optical properties, confinement, edge effects

Date Published: 12/20/2016

Citation: Backes, C., Hanlon, D., Szydlowska, B.M., Harvey, A., Smith, R.J., Higgins, T.M., Coleman, J.N. Preparation of Liquid-exfoliated Transition Metal Dichalcogenide Nanosheets with Controlled Size and Thickness: A State of the Art Protocol. *J. Vis. Exp.* (118), e54806, doi:10.3791/54806 (2016).

Abstract

We summarize recent advances in the production of liquid-exfoliated transition metal dichalcogenide (TMD) nanosheets with controlled size and thickness. Layered crystals of molybdenum disulphide (MoS_2) and tungsten disulphide (WS_2) are exfoliated in aqueous surfactant solution by sonication. This yields highly polydisperse mixtures containing nanosheets with broad size and thickness distributions. However, for most purposes, specific sizes (in terms of both lateral dimension and thickness) are required. For example, large and thin nanosheets are desired for (opto) electronic applications, while laterally small nanosheets are interesting for catalytic applications. Therefore, post-exfoliation size selection is an important step that we address here. We provide a detailed protocol on the efficient size selection in large quantities by liquid cascade centrifugation and the size and thickness quantification by statistical microscopic analysis (atomic force microscopy and transmission electron microscopy). The comparison of MoS_2 and WS_2 shows that both materials are size-selected in a similar way by the same procedure. Importantly, the dispersions of size-selected nanosheets show systematic changes in their optical extinction spectra with size due to edge and confinement effects. We show how these optical changes are related quantitatively to the nanosheets dimensions and describe how mean nanosheets length and layer number can be extracted reliably from the extinction spectra. The exfoliation and size selection protocol can be applied to a broad range of layered crystals as we have previously demonstrated for graphene, gallium sulphide (GaS) and black phosphorus.

Video Link

The video component of this article can be found at https://www.jove.com/video/54806/

Introduction

The possibility to produce and process graphene, related two-dimensional (2D) crystals in the liquid phase makes them promising materials for an ever growing range of applications as composite materials, sensors, in energy storage and conversion and flexible (opto) electronics.[1-6] To exploit 2D nanomaterials within applications such as these will require inexpensive and reliable functional inks with on-demand lateral size and thickness of the nanoscale constituents, as well as controlled rheological and morphological properties amenable to industrial-scale printing/coating processes.[7] In this regard, liquid phase exfoliation has become an important production technique giving access to a whole host of nanostructures in large quantities.[6,8,9] This method involves the sonication or shearing of layered crystals in liquids. If the liquid is appropriately chosen (*i.e.,* suitable solvents or surfactant) the nanosheets will be stabilized against reaggregation. Numerous applications and proof-of-principle devices have been demonstrated by such techniques.[6] Probably the greatest strength of this strategy is its versatility, as numerous layered parent crystals can be exfoliated and processed in a similar way, providing access to a broad palette of materials which can be tailored to the desired application.

However, despite this recent progress, the resultant polydispersity that arises due to these liquid-phase production methods (in terms of nanosheet length and thickness) still presents a bottleneck in the realization of high performance devices. This is mostly because the development of novel and innovative size selection techniques has thus far required nanosheets length and thickness characterization using tedious statistical microscopy (atomic force microscopy, AFM and/or transmission electron microscopy, TEM).

Despite these challenges, several centrifugation techniques have been reported to achieve length and thickness sorting.[6,10-13] The simplest scenario is homogeneous centrifugation, where the dispersion is centrifuged at a given centrifugal acceleration and the supernatant is decanted for analysis. The centrifugation speed sets the size cut-off, whereby the higher the speed, the smaller are the nanosheets in the supernatant. However, this technique suffers from two major disadvantages; firstly, when larger nanosheets are to be selected (*i.e.,* the dispersion is centrifuged at low speeds and the supernatant is decanted) all smaller nanosheets will also remain in the sample. Secondly, regardless of the centrifugation speed, a significant proportion of the material tends to be wasted in the sediment.

An alternative strategy for size selection is density gradient (or isopycnic) centrifugation.[11,14] In this case, the dispersion is injected into a centrifuge tube containing a density gradient medium. During ultracentrifugation (typically > 200,000 x g), a density gradient is formed and the nanosheets move to the point in the centrifuge where their buoyant density (density including the stabilizer and solvent shell) matches the density of the gradient. Note that the nanomaterial can also move upward during this process (depending on where it was injected). In such a way, the nanosheets are effectively sorted by thickness rather than mass (opposed to homogeneous centrifugation). While this procedure offers a unique opportunity to sort nanosheets by thickness, it suffers from notable disadvantages. For example, the yields are very low and at present do not allow for the mass production of separated nanosheets. This is partly related to low contents of monolayers in stock dispersions after liquid-exfoliation and can potentially be improved by optimizing exfoliation procedures in the future. In addition, it is typically a time-consuming multi-step ultracentrifugation process involving multiple iterations to achieve efficient size selection. Furthermore, in the case of inorganic nanomaterials, it is restricted to polymer-stabilized dispersions to obtain the required buoyant densities and the gradient medium in the dispersion may interfere with further processing.

We have recently shown that a procedure we term liquid cascade centrifugation (LCC) offers an exciting alternative,[13] as we will also detail in this manuscript. This is a multi-step procedure which is extremely versatile allowing various cascades to be designed according to the desired outcome. To demonstrate this process, a standard cascade is portrayed in **Figure 1** and involves multiple centrifugation steps whereby each features a higher speed than the last. After each step, the sediment is retained and the supernatant is then used in the proceeding stage. As a result, each sediment contains nanosheets in a given size range which have been "trapped" between two centrifugations with different speeds; the lower one removing larger nanosheets into the previous sediment while the higher speed removes the smaller nanosheets into the supernatant. Critical to LCC, the resulting sediment can be redispersed completely by mild sonication in the respective medium, which in this case is aqueous sodium cholate H_2O-SC (at SC concentrations as low as 0.1 g L^{-1}). The result is dispersions with virtually any chosen concentration. Importantly, virtually no material is wasted in LCC, resulting in the collection of relatively large masses of size-selected nanosheets. As shown here, we have applied this procedure to a number of liquid-exfoliated nanosheets including MoS_2 and WS_2 as well as GaS,[15] black phosphorus[16] and graphene[17] in both solvent and surfactant systems.

This unique centrifugation procedure enables the efficient size-selection of liquid exfoliated nanosheets and has subsequently enabled a significant advancement in terms of their size and thickness determination. In particular, through this approach we demonstrated previously that optical extinction (and absorbance) spectra of the nanosheets change systematically as function of both nanosheets lateral dimensions and nanosheets thickness. As we summarize here, this has allowed us to link the nanosheet spectral profile (specifically the intensity ratio at two positions of the extinction spectrum) to the mean nanosheet length as a result of nanosheet edge effects.[12,13] Importantly, the same equation can be used to quantify the size of MoS_2 and WS_2. Furthermore, we show that the A-exciton position shifts towards lower wavelengths as a function of mean nanosheet thickness due to confinement effects. Even though exfoliation, as well as size selection and determination are in general rather robust procedures, the quantitative outcome depends on subtleties in the protocol. However, especially for newcomers to the field, it is difficult to judge which process parameters are most relevant. This comes down to the fact that experimental sections of research papers only provide a rough protocol, without discussing what outcome is to be expected when modifying the procedure or giving a rational behind the protocol. In this contribution, we intend to address this as well as provide a detailed guide and discussion to the production of liquid-exfoliated nanosheets of controlled size and to the accurate determination of size by either statistical microscopy or analysis of the extinction spectra. We are convinced that this will help to improve reproducibility and hope it will be a useful guide for other experimentalists in this research area.

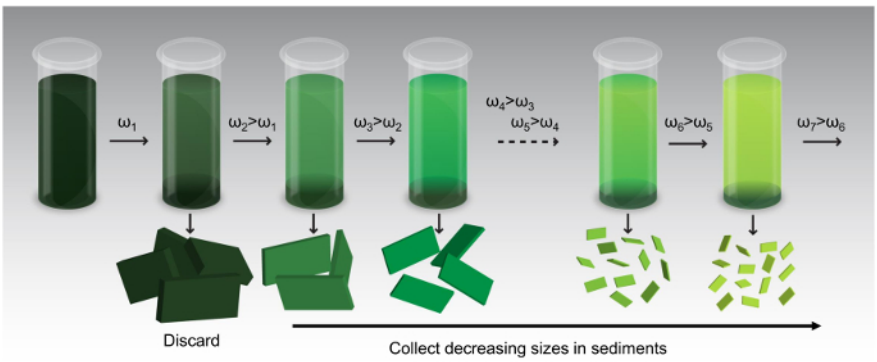

Figure 1: Schematic of the size selection by liquid cascade centrifugation. Size-selected nanosheets are collected as sediments. Each sediment is collected or "trapped" between two centrifugation speeds (ω) starting from low speeds and going to higher ones from step to step. The sediment discarded after the first centrifugation contains unexfoliated layered crystallites while the supernatant discarded after the last centrifugation step contains extremely small nanosheets. Size-selected dispersions are prepared by re-dispersing the collected sediments in the same medium (here aqueous surfactant solution) at reduced volumes. Adapted with permission from [13]. Please click here to view a larger version of this figure.

Protocol

1. Liquid Exfoliation — Preparation of Suitable Stock Dispersions

1. Mount a metal cup underneath a sonotrode in an ice bath.
2. Immerse 1.6 g of the TMD powder in 80 mL aqueous solution of sodium cholate (SC) surfactant (sodium cholate concentration, C_{SC}= 6 g L^{-1}) in the metal cup.
3. Move the sonic tip to the bottom of the metal cup and then up by ~ 1 cm. Wrap aluminum foil around the sonic probe to avoid spillage.

4. Sonicate the mixture under ice-cooling by probe sonication to avoid heating using a solid flathead tip (750 W processor) for 1 h at 60% amplitude (pulse of 6 s on and 2 s off).
5. Centrifuge the dispersion at a centrifugation speed of 2,660 x g for 1.5 h. Discard the supernatant containing impurities and collect the sediment in 80 mL fresh surfactant solution (C_{SC}= 2 g L^{-1}).
   NOTE: Use maximum filling heights in the centrifuge tubes of maximum 10 cm. Otherwise, increase the centrifugation time.
6. Subject the dispersion to a second, longer sonication using the solid flathead tip for 5 h at 60% amplitude (pulse of 6 s on and 2 s off) under ice-cooling. Replace the ice bath every 2 h while pausing the sonication.

2. Nanosheet Size Selection by Liquid Cascade Centrifugation

NOTE: To select nanosheets by size, liquid cascade centrifugation with sequentially increasing centrifugal acceleration is applied (**Figure 1**). The following procedure is recommended as standard size selection of the cascade in the case of TMDs. For other materials, centrifugation speeds may need to be adjusted.

1. Remove unexfoliated powder by centrifugation at 240 x g (1.5 krpm), 2 h. Discard the sediment.
2. Centrifuge the supernatant at a higher centrifugal acceleration: 425 x g (2 krpm), 2 h. Collect the sediment in fresh surfactant at reduced volume (3-8 mL).
3. Centrifuge the supernatant at even higher centrifugal acceleration: 950 x g (3 krpm), 2 h. Collect the sediment in fresh surfactant at reduced volume (3-8 mL).
4. Repeat this procedure with the following centrifugal accelerations: 1,700 x g (4 krpm), 2,650 x g (5 krpm), 3,500 x g (6 krpm), 5,500 x g (7.5 krpm), and 9,750 x g (10 krpm).

3. Determination of Nanosheets Size and Thickness by Statistical Microscopy

NOTE: If spectroscopic metrics are already available, section 3 can be skipped or reduced, *i.e.,* not carried out for every sample.

1. Length: Transmission electron microscopy (TEM)
   1. Deposition
      1. Dilute the high concentration dispersions with water (to reduce the surfactant concentration) so that they are of light in color. Drop cast onto a grid (for example holey carbon, 400 mesh) placed on a filter membrane to wick away excess solvent.
   2. Imaging
      1. Record multiple images on different positions on the grid. Adjust the field of view depending on nanosheet size. For a comprehensive TEM imaging tutorial, see reference [18].
   3. Statistical length analysis performed using ImageJ
      1. Open the ImageJ software, select the relevant TEM image via the "file" menu and "open" the image. The image will open in a new window.
      2. Click the "analyze" tab. Select "set scale" from the drop down menu. A new window will open. Click "remove scale", tick "global" and click "ok".
      3. Select the "line" tool. Draw a line profile along the length of the scale bar of the TEM image.
      4. Click "analyze". Select "set scale" from the drop down menu. Enter the length of the scale bar in nm into the "known distance" box and click "ok".
         NOTE: The distance of the line drawn on the scale bar is displayed in pixels.
      5. Select the "line" tool and measure the nanosheet length by drawing a line profile of the longest axis of the nanosheet.
      6. Press "control+M" to measure. A new box labelled "results" opens with the nanosheet length displayed in the "length" column.
      7. Repeat step 3.1.3.6 for all individually deposited nanosheets (not aggregated ones) in the image.
      8. When opening a new image, repeat steps 3.1.3.3- 3.1.3.7. Count the length of 150 nanosheets.
         NOTE: All nanosheet length data is compiled in the "results" window and can be copied into other programs for further processing.

2. Thickness: Atomic force microscopy (AFM)
   1. Dilute the dispersion so that are almost transparent to the human eye (corresponding to extinction intensity of ideally ~0.2 per 1 cm pathlength at 400 nm). In the case of surfactant dispersions, dilute with water not surfactant.
   2. Drop-cast on pre-heated wafers. For water-based dispersion, heat the wafer to ~170 °C on a hot plate and deposit 10 µL per 0.5 x 0.5 cm^2 wafer.
   3. Rinse the wafers thoroughly with a minimum of 5 mL of water and 3 mL of 2-propanol to remove residual surfactant and other impurities.
   4. Scan and save multiple images across the sample with the AFM in tapping mode. For small nanosheets use a resolution of 512 lines per image and image sizes of maximum 2 x 2 $µm^2$. For samples containing larger nanosheets, increase the field of view to up to 8 x 8 $µm^2$. Use scan rates as appropriate (typically 0.4-0.7 Hz). Alternatively, scan larger areas at higher resolution.
   5. Thickness measurement using Gwyddion Software
      1. Open the software and select the relevant AFM image via "file" and "open". The image will open in a new window.
      2. Correct the background using the "level data by mean plane subtraction" "align rows" and "correct horizontal scars" in the "Data Process" section of the home menu. Apply the corrections, change the image color for better contrast by right-clicking on the legend and set z-plane to zero.
      3. Zoom in the region of choice (if convenient). Click on the "crop" tool in the home menu. Drag the cursor over the image to mark the region of choice. Press "apply". Check the "create new channel" to open the selected region in a new window.

4. Select "extract profiles" from the tools menu. A new window opens.
5. Draw a line across the nanosheet. Write down the thickness in a table. In the case of non-homogeneously thick nanosheets, average the thickness across the nanosheet. Take extreme care to measure only individually deposited and non-aggregated nanosheets.
6. Repeat 3.2.5.3-3.2.5.5 for all nanosheets on the image.
7. Repeat 3.2.5.1-3.2.5.6 for all images recorded. Count minimum 150 nanosheets.

3. Conversion of AFM thickness to layer number
NOTE: Apparent AFM heights from liquid exfoliated nanomaterials are usually overestimated due to the presence of residual solvent. In addition, accurate height measurements of inhomogeneous samples (such as nanomaterials deposited on substrates) using AFM are generally challenging due to contributions from effects such as capillary forces and adhesion which depend on the material and measurement parameters.[19,20] To overcome these problems and to convert the apparent measured AFM thickness to the number of layers, a procedure termed step height analysis was developed as described in the following.[12,13,16,21]. Steps 3.3.1-3.3.4 can be skipped if the step height is known.
1. Open, correct and crop the AFM image as described in 3.2 to select a nanosheet with clearly discernible terraces.
2. Measure the height across the nanosheet using the "extract" profile tool.
NOTE: Suitable profiles show discrete steps as the one in **Figure 2B** inset.
1. Record the height of these steps (*i.e.,* the height difference from one terrace to the next on the nanosheet).
3. Count at least 70 of these steps.
4. Plot the step height in ascending order (**Figure 2C**).
NOTE: Observe that for TMDs the apparent step height is always a multiple of ~1.9 nm.
5. Divide the apparent AFM thickness (measured as described in section 3.2) by 1.9 nm to obtain the layer number.
NOTE: Other materials have other step height conversion factors requiring a different calibration.

4. Determination of MoS_2 and WS_2 Size and Thickness Based on Extinction Spectra

1. Spectra acquisition
1. Dilute the high concentration samples with the respective medium (here aqueous sodium cholate, 2 g L^{-1}) to yield extinctions below 2 across the entire spectral range.
2. Set the increments for the spectral acquisition to 0.5 nm in the instrument settings or use scan speed slow or medium.
3. Choose the settings "subtract baseline" in the instrument settings. Place the cuvette containing the aqueous sodium cholate solution in the sample compartment of the spectrometer and run the measurement.
4. Remove the cuvette with the sodium cholate solution from the spectrometer and empty it. Fill in the sample, place the sample in the sample compartment of the spectrometer and run a scan of the sample.

2. Length determination from intensity ratios
1. Option 1: Read-off the intensity at the A-exciton, Ext_A (~660 nm for MoS_2 and 620 nm for WS_2) and the local minimum Ext_{min} (345 nm for MoS_2 and 295 nm for WS_2). Divide the intensity at the A-exciton by the intensity at the local minimum to obtain the intensity ratio Ext_A/Ext_{min}.
2. Determine the mean nanosheet length, <L> by using equation 1.

$$< L > = \frac{1000\frac{Ext_A}{Ext_{Min}} - 7.6}{2.8} \quad \text{(Eq. 1)}$$

where Ext_A/Ext_{min} is the intensity ratio of the extinction at the A-exciton (Ext_A) and the local minimum (Ext_{min}).
NOTE: The equation holds for both MoS_2 and WS_2. However, its accuracy is limited especially for small nanosheets.
3. Option 2: Determine the intensity ratio of the local maximum in the UV region of the spectrum, $Ext_{Max\text{-}HE}$ (270 nm for MoS_2 and 235 nm for WS_2) and the local minimum, Ext_{min} (345 nm for MoS_2 and 295 nm for WS_2)
4. Determine the mean nanosheet length, <L> by using equation 2.

$$< L > = \frac{2.3 - \frac{Ext_{Max-HE}}{Ext_{Min}}}{0.02\frac{Ext_{Max-HE}}{Ext_{Min}} - 0.0185} \quad \text{(Eq. 2)}$$

With $Ext_{max\text{-}HE}$ denoting the intensity at the local maximum at high energy (270 nm for MoS_2 and 235 nm for WS_2) and Ext_{min} the extinction intensity at the local minimum (345 nm for MoS_2 and 295 nm for WS_2).
NOTE: Option 2 gives a more accurate measure of the lateral size. However, the high energy region may not be accessible in all solvents/surfactant.

3. Concentration
1. Record the extinction intensity relative to 1 cm pathlength at 345 nm for MoS_2 and 235 nm for WS_2, respectively.
NOTE: Divide the recorded measured extinction by the pathlength of the cuvette.
2. Divide this intensity by the extinction coefficients of 68 $Lg^{-1}cm^{-1}$ at 345 nm for MoS_2 and 47 $Lg^{-1}cm^{-1}$ at 235 nm for WS_2 to obtain the nanosheet concentration in gL^{-1}.

4. Thickness determination from A-exciton position
1. Calculate the second derivative of the spectrum.

1. Using the data analysis and graphing software (*e.g.,* OriginPro), select the column containing the extinction intensity. Click on the "analysis" tab, select "mathematics" from the drop down menu and "differentiate", "open dialog". A new window will open. Set the derivative order to 2 and press ok.

2. Smooth the second derivative by Adjacent Averaging (~ 10-20 points per window in A-exciton region).
    1. For example, using the data analysis and graphing software, plot the second derivative spectrum.
        1. With the graphic window active, click on "analysis" and choose "signal processing", then "smooth" then "open dialog" from the drop down menu. A new window will open.
        2. Choose "Adjacent Averaging" as smoothing method and set the points to 20.
        3. Plot the resultant smoothed spectrum which is displayed as new columns. If the noise is still high, repeat the smoothing. NOTE: Usually, spectral smoothing is required to reduce the noise unless high integration times during the measurement are used. The appropriate smoothing is an important part of the data analysis and the appropriate smoothing method depends on the desired outcome. This particular smoothing method is only ideal to determine the mean peak position.[13]

3. Read-off the peak position from the second derivative. This is the wavelength of the A-exciton, λ_A. Alternatively, carry out the steps described in 4.4.4-4.4.7.
4. Convert the x-axis from wavelength to energy using the relation:
   E(eV) = 4.135E-6 * 2.997E8 / λ(nm)
5. Fit the second derivative to the second derivative of a Lorentzian.
   NOTE: A Lorentzian can be written as

$$L = \frac{h}{\left[1+\left(\frac{(E-E_0)}{w/2}\right)^2\right]} \quad \text{(Eq. 3)}$$

   Where *h* is the height, E'_0 is the center and *w* is the FWHM. Differentiating twice with respect to *E* gives

$$\frac{d^2L}{dE^2} = -\frac{8h}{w^2}\left[\frac{1-3\left(\frac{E-E_0}{w/2}\right)^2}{\left(1+\left(\frac{E-E_0}{w/2}\right)^2\right)^3}\right] \quad \text{(Eq. 4)}$$

    1. In the data analysis and graphing software, choose "tools" from the main menu and select "fitting function builder". A new window will open.
    2. Select "create a new function", click next.
    3. Leave the default settings, give the function a name and click next.
    4. Set "h,E,w" as parameters, click next.
    5. Enter "(-8*h/w^2)*(1-3*(2*(E-x)/w)^2)/(1+(2*(E-x)/w)^2)^3" as function body, click finish.
    6. Plot only the A-exciton region of the second derivative spectrum on the energy scale.
    7. With the graphics window active, click on the "analysis" tab. Choose "fitting", "nonlinear curve fit", "open dialog" from the drop down menu. A new window will open.
    8. Select "user defined" in category and choose the previously built function in the function box. In the tab "parameters" set initial values for w to 0.1, and E to 1.99 for WS_2 and 1.85 for MoS_2. Press "fit"

6. Record the energy E'_0, which is the energy associated with the A-exciton, E'_A.
7. Determine the number of layers according to equations 5 (MoS_2) and 6 (WS_2).

$$N = 2.3\times10^{36} e^{-54888/\lambda_A} = 2.3\times10^{36} e^{-44.3E_A} \quad \text{(Eq. 5, } MoS_2\text{)}$$

$$N = 6.35\times10^{-32} e^{\lambda_A/8.51} = 6.35\times10^{-32} e^{146/E_A} \quad \text{(Eq. 6, } WS_2\text{)}$$

   with λ_A denoting the wavelength of the A-exciton and E_A denoting the energy of the A-exciton.

Representative Results

Liquid cascade centrifugation (**Figure 1**) is a powerful technique to sort liquid-exfoliated nanosheets by size and thickness as illustrated in **Figure 2** for both MoS_2 and WS_2. Nanosheet lateral sizes and thicknesses can be characterized by statistical TEM and AFM, respectively. A typical AFM image is shown in **Figure 2A**. The apparent nanosheet thickness is converted to layer number using step height analysis (**Figure 2B** and **C**). Statistical microscopic analysis yields length and number of layer histograms such as presented in **Figure 2D** and **E**, respectively. This analysis over a broad number of fractions produced from LCC is used to characterize the size selection process. In **Figure 2F** and **G**, the mean nanosheet length and layer number is plotted as function of central acceleration of the LCC. A similar trend is observed for both MoS_2 and WS_2. To gain further insights in both exfoliation and size selection, the length is plotted as function of nanosheet layer number in **Figure 2H** showing well-defined relationships confirming that smaller, thinner nanosheets are separated from larger, thicker ones.

Even though microscopy statistics are an important foundation to characterize the size-selection process, they suffer from the drawback that they are extremely time consuming. Alternatively, optical extinction spectra can be used to quantify both length and thickness. This is illustrated in **Figure 3**. **Figure 3A** and **C** show optical extinction spectra of MoS_2 (A) and WS_2 (C) with different mean nanosheet sizes and thicknesses. **Figures 3B** and **D** show the corresponding fitted second derivatives of the A-exciton region of both materials illustrating well-defined peak shifts of the transition.

One way to express spectral changes is *via* peak intensity ratios at fixed spectral positions. If these are chosen with care, they can be related to the mean nanosheet length as shown in **Figure 3E, F**. Interestingly, data for MoS_2 and WS_2 collapses on the same curve if appropriate peak positions are chosen. For example, peak intensities of the A-exciton over the local minimum Ext_A/Ext_{min} follow the same trend for both materials (**Figure 3E**), as well as the peak intensity ratio at the high energy maximum over the local minimum $Ext_{Max\text{-}HE}/Ext_{min}$ (**Figure 3F**). This means that the nanosheet size for both materials can be quantitatively linked to the nanosheet length *via* the same equations (Eq. 1 and 2). Due to the changes in spectral shape, extinction coefficients are also dependent on nanosheet size. This is more or less severe depending on the spectral position. For example, as plotted in **Figure 3G**, the extinction coefficient of the A-exciton for both materials is strongly length dependent. However, this is not the case at 345 nm for MoS_2 and 235 nm for WS_2 so that the extinction coefficient at these spectral positions can be used as a reasonably robust measure for nanosheet concentration over a broad range of sizes. In addition, extinction spectra do not only provide insight in nanosheet lateral size and dispersed concentration, but also in nanosheet thickness. The number of layers can be quantitatively related to the peak position/energy of the A-exciton (obtained from an analysis of the second derivative) as plotted in **Figure 3H**.

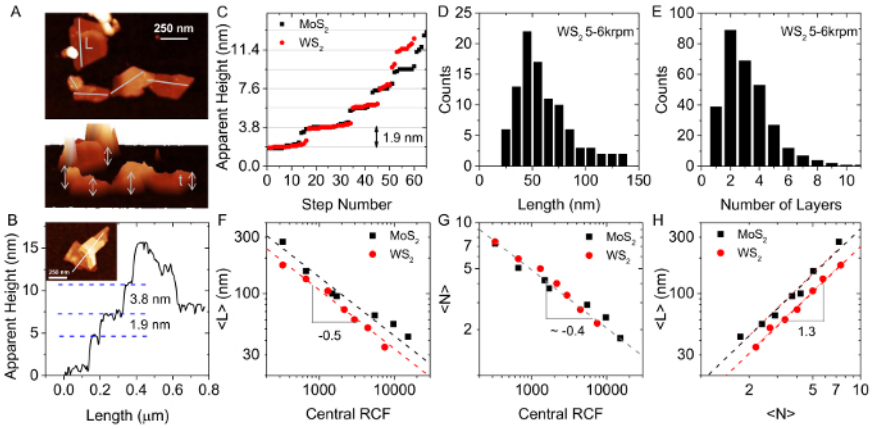

Figure 2: Size determination and result of the LCC size selection for MoS_2 and WS_2. A) Representative AFM image of individually deposited nanosheets in two-dimensional (top) and three-dimensional (bottom) view. From such images, nanosheet length, *L* and apparent AFM height, *i.e.,* thickness, *t* is determined. **B**) Image (inset) and line profile across an inhomogeneously exfoliated nanosheet. Steps associated with terraces on the nanosheet are clearly discernable. **C**) Step heights of nanosheets such as in B plotted in ascending order. For both MoS_2 and WS_2, these are always a multiple of 1.9 nm. This means one layer has an apparent AFM thickness of 1.9 nm. **D**) Histogram of nanosheet length of a representative sample from statistical TEM. **E**) Number of layer, *N*, histogram of the sample in D. *N* was determined by dividing the apparent thickness by the step height of 1.9 nm. **F, G**) Mean nanosheet length <*L*> (**F**) and number of layers <*N*> (**G**) plotted as a function of central RCF in the LCC. **H**) Plot of nanosheet length as a function of thickness for size-selected MoS_2 and WS_2. Adapted with permission from [12,13]. Please click here to view a larger version of this figure.

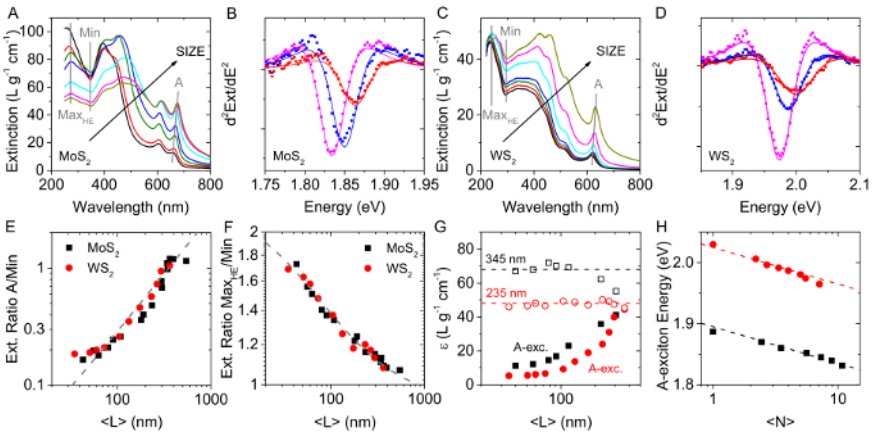

Figure 3: Extinction spectra and spectroscopic size and thickness metrics. A, C) Optical extinction spectra of LCC separated MoS_2 (**A**) and WS_2 (**C**). Peaks relevant for the analysis are indicated. **B, D**) Second derivatives of the A-exciton plotted *versus* energy for MoS_2 (**B**) and WS_2 (**D**) after smoothing the second derivative with Adjacent Averaging. The solid lines are fits to the second derivative of a Lorentzian to assess peak positions/energies. **E, F**) Plots of peak intensity ratios as a function of mean nanosheet length <*L*>. Data for MoS_2 and WS_2 falls on the same curve. Hence the same equations can be used to quantify nanosheet length. **E**) Plot of the peak intensity ratio at the A-exciton / local minimum. <*L*> can be determined according to equation 1. **F**) Plot of the peak intensity ratio at the high energy maximum / local minimum. <*L*> can be determined according to equation 2. **G**) Extinction coefficient at different spectral positions as function of nanosheet length. At some spectral positions (such as the A-exciton), extinction coefficients are highly size dependent, while at others (345 nm for MoS_2 and 235 nm for WS_2) this is not the case. **H**) Plot of A-exciton peak energies (from second derivatives) plotted as function of layer number <*N*>. Layer numbers can be determined according to equations 5 and 6. Adapted with permission from [12,13]. Please click here to view a larger version of this figure.

Discussion

Sample preparation

The samples described here are produced by tip sonication. Alternative exfoliation procedures can be used, but will lead to different concentrations, lateral sizes and degrees of exfoliation. Higher amplitudes and longer on pulses during the sonication should be avoided to prevent damaging of the sonicator. Similar results were obtained using 500 W processors. However, sonication time and amplitude has an impact on the nanosheet exfoliation and variations from this protocol may result in different nanosheet sizes and concentrations than presented here. We emphasize that cooling is critical during the sonication, as heating can damage and degrade the nanosheets and deteriorate the resulting optical properties of the material obtained. While higher initial concentrations of the TMD powder can increase the nanosheet concentration beyond that obtained here, this does not occur linearly. For tip-sonication, the dispersed concentration typically saturates beyond initial TMD concentrations of 30-40 gL^{-1}.

The chosen size-selection cascade can be modified readily to suit a desired outcome. While this specific procedure yields nanosheet sizes and thicknesses over a broad size range in the different fractions, if only specific sizes are targeted the centrifugation steps can be skipped. For instance, if medium-sized nanosheets are desired, the sample can be centrifuged at only two different centrifugal accelerations and the sediment redispersed. Alternatively, more complex cascades can be applied to achieve monolayer enrichment (see [13] for further clarification). This flexibility in combination with the ability to redisperse the samples at high concentrations is a unique advantage of LCC over other size-selection protocols.

It is recommended to use filling heights in the centrifuge vials of < 10 cm for this protocol. If larger filling heights in the vials are used, the centrifugation times need to be increased to obtain comparable results. The sediment should always be pellet-like for efficient size selection and the supernatant decanted carefully and completely. If the sediment is not pellet-like, the centrifugation time needs to be increased. Higher temperatures (also during the centrifugation) should be avoided and samples are best stored in the refrigerator to minimize material degradation after preparation. If the centrifugation is carried out at lower temperatures, sedimentation is slower and centrifugation times may require adjustment. Different centrifuge and rotor geometries may result in length and thickness deviations from the representative data shown. However, despite these subtleties, in general, the size selection procedure is robust and can be applied to various materials in solvents as well as surfactants. The final supernatant after centrifugation at high accelerations is typically discarded, as it contains very small (< 30 nm) nanosheets with properties dominated by edges only. The size selection scheme can be carried out in any benchtop centrifuge (*i.e.*, no ultracentrifuge is required opposed to density gradient centrifugation). Here, all centrifugations were performed at 15 °C for 2 h in each step using the 220R centrifuge (see Materials List). Two different rotors were used; for speeds ≤ 3,500 x g, a fixed angle rotor was employed where the centrifugation rate, *f* (in krpm) is related to the centrifugal force *via* $RCF = 106.4\ f^2$. In this case, 28 mL glass vials containing ~10 mL aliquots = 10 cm filling height were used. For speeds > 3,500 x g, samples were centrifuged in 1.5 mL plastic centrifuged tubes in a fixed angle rotor, where *f* is related to the centrifugal force *via* $RCF = 97.4\ f^2$.

For the analysis of the nanosheet length, TEM is recommended as analysis tool due to the higher resolution compared to scanning electron microscopy and the higher throughput compared to AFM. Furthermore, AFM also has the disadvantage that lateral sizes are typically overestimated due to tip broadening and pixilation. Any conventional TEM even with acceleration voltages of 200 kV can be used. In this case, imaging was performed on holey carbon grids (400 mesh). For very small nanosheets, continuous film grids can be beneficial but are not required. In turn, AFM is recommended as analysis tool to determine nanosheet layer number. This is because TEM thickness determination by edge counting can be problematic, as nanosheets become thinner towards the edge, necessitating that multiple regions for each nanosheet

would need to be inspected to determine the mean thickness. This is much less problematic when using AFM as the measured thickness is readily averaged over inhomogeneous nanosheets. For AFM analysis it is particularly critical to avoid re-aggregation of nanosheets on the wafer during solvent evaporation. To avoid this, it is recommended that the dispersion is drop-cast on pre-heated wafers. The water-carrier immediately evaporates and bubbles are formed, resulting in more uniform deposition compared to drop casting on wafers at lower temperature. Si/SiO_2 wafers with 200-300 nm oxide layer are recommended as nano-scaled objects can be seen with an optical microscope/optical zoom as blue spots.[22] This is a useful guide to allocate regions of interest for imaging. The field of view should be adjusted according to nanosheet size. For the data presented here, AFM was carried out on 13 µm scanner in tapping mode. Typical image sizes ranged from 2 x 2 μm^2 to maximum 8 x 8 μm^2 for the larger nanosheets at scan rates of 0.4-0.7 Hz with 512 lines per image. Alternatively, depending on the specific AFM or scanner, scanning of larger areas at a higher resolution (*e.g.,* up to 16 x 16 μm^2 with 1,024 lines) could be convenient. A typical image is shown in **Figure 2A, B**. Residual surfactant can make the thickness measurements very tedious especially for very small nanosheets that are more difficult to distinguish from surfactant. In this case, phase images can provide a guide, as they usually give a good contrast between different materials. If problems with residual surfactant persist, the wafers can be soaked in water overnight without significant loss of the nanosheets on the wafer.

In general, counting less than 150-200 nanosheets may be sufficient for samples with smaller mean size, as these tend to be less polydisperse. If a non-size-selected stock dispersion is analyzed, it is recommended that at least 200 nanosheets should be recorded. If solvents are used throughout the procedure instead of surfactant/water solutions, the dispersions have to be diluted with the respective solvent prior to deposition. Care must be taken during imaging not to bias the counting towards larger nanosheets, which are easier to discern. The concentration of the deposited dispersions is important as nanosheets tend to re-aggregate for excessive nanosheet concentrations, leading to inaccurate size/thickness determination. Outliers towards extreme nanosheet sizes on either the larger or smaller end can bias the statistics dramatically. In extreme cases, these should not be included in the determination of the mean values. Histograms are typically log-normal in shape[23] (**Figure 2D, E**). If this is not the case, the counting and/or imaging may be biased. From these histograms and the statistical analysis, the arithmetic number mean is obtained. This is typically also related to the volume fraction weighted mean value and therefore a valid measure of lateral size/thickness.

Size selection and metrics

Both mean nanosheet length, $\langle L \rangle$ and nanosheet thickness, $\langle N \rangle$ are reduced as the centrifugation rates are increased, *i.e.,* as the dispersion progresses through the cascade. We can quantify these effects by plotting $\langle L \rangle$ (from TEM) as a function of the centrifugal acceleration (RCF) associated with the midpoint of centrifugation rates denoted as central RCF (**Figure 2F**). The mean nanosheet length falls off as $(\text{central RCF})^{-0.5}$ for both MoS_2 and WS_2. At the same central centrifugal accelerations, the lateral sizes of MoS_2 are slightly larger than for WS_2 which is attributed to the lower density of the material. Similarly, $\langle N \rangle$ (from AFM statistics) is plotted *versus* central RCF in **Figure 2G**. It falls with central rotational speed *via* $(\text{central RCF})^{-0.4}$. Interestingly, the data from MoS_2 and WS_2 roughly collapses on the same curve. Reasons for this behavior are currently not understood and require further exploration. In conclusion, smaller and thinner nanosheets are separated from larger and thicker ones as illustrated in **Figure 2H**.

Even though this may be expected from centrifugation, we note that this is not necessarily related to the centrifugation process alone. This is also because we consistently find for a number of materials exfoliated by sonication (MoS_2[12], WS_2[13], MoO_3[24], black phosphorus[16], GaS[15]) that thinner nanosheets tend to be smaller, while thicker nanosheets tend to be larger. An analysis of the lateral dimensions for nanosheets of a given thickness in each fraction previously showed that the mean length of the nanosheet is roughly constant within one sample for different thicknesses.[13] This is interesting, as it implies that this centrifugation is a length separation process in first approximation. This suggests that equilibrium in the centrifugation is not reached after the relatively short centrifugation times of 2 h in each step so that, back diffusion and friction can play a prominent role. This also means that different nanosheet length-thickness relations can be produced by modifying the cascade.[13]

The spectral profile of optical extinction spectra strongly depends on nanosheets dimensions due to edge and confinement effects. Here we use the fractions produced by LCC to investigate the effect of nanosheet size and thickness on the extinction spectra of MoS_2 and WS_2. Extinction spectra measured in standard transmission contain contributions from both absorbance and scattering.[12,25] Absorbance spectra can be obtained by a measurement in the center of an integrating sphere where all scattered light is collected. In the resonant regime, *i.e.*, where the nanomaterial absorbs light, the scattering spectrum follows the absorbance roughly in shape. Therefore, information encoded in an absorbance spectrum can be obtained from an analysis of extinction spectra.[12,13,15-17] In the non-resonant regime (above ~ 700 nm for MoS_2 and WS_2), the scattering exponent can be determined which is also related to the nanosheet (lateral) size. See references [12,13,15-17].

As shown in **Figure 3A** and **C**, optical extinction spectra display the characteristic excitonic transitions,[26] but vary systematically with nanosheet size and thickness. In addition to variations in relative intensities across the entire spectral regions, shifts of the excitonic transitions are observed. This is best visualized from the second derivative spectra in the region of the A-exciton (**Figure 3B** and **D**).

Edge effects result in a dependence of the spectral profile on nanosheet length.[12] The changes in spectral shape with nanosheet lateral size can be rationalized by edges being electronically different from center regions. Therefore, the extinction coefficient associated with the nanosheet edge is different from extinction coefficients at the basal planes. This can be quantified *via* the ratio of extinction intensities at two different wavelengths. In principle, any peak intensity ratio can be related to the nanosheet size. However, the size metrics will be more reliable the larger the difference in the spectral shape at the given positions. Suitable examples are intensity ratios at the A-exciton to that at the local minima, Ext_A/Ext_{min} (**Figure 3E**) or at the high-energy maxima to that at the local minima, $Ext_{Max\text{-}HE}/Ext_{min}$, (**Figure 3F**).

The data in **Figures 3E, F** can be fitted to the following equation[12]

$$\frac{Ext_{\lambda 1}}{Ext_{\lambda 2}} = \frac{\varepsilon_c(\lambda 1)L + 2x(k+1)\Delta\varepsilon(\lambda 1)}{\varepsilon_c(\lambda 2)L + 2x(k+1)\Delta\varepsilon(\lambda 2)} \quad \text{(Eq. 7)}$$

Where ε_c is the extinction coefficient associated with the nanosheet basal plane, $\Delta\varepsilon = \varepsilon_E - \varepsilon_c$ where ε_E is the edge region extinction coefficient, and L, x and k are the nanosheet length, edge thickness and length-width aspect ratio, respectively. We find this equation fits the data very well allowing us to generate functions relating the mean nanosheet length, L to the extinction peak intensity ratios (see equations 1 and 2). The

intensity ratio Ext_A/Ext_{min} is extremely useful, as it can also be applied to solvent systems, where the solvent itself absorbs light in the UV region. However, it is less accurate and breaks down for smaller nanosheets. It is therefore recommended to use equation 2 involving Ext_{Max-HE}/Ext_{min} when the UV region is accessible.

As a result of these edge effects, extinction coefficients change as a function of nanosheet size (**Figure 3G**) making accurate concentration measurements of the nanosheets in the dispersion challenging. However, for both MoS_2 and WS_2, we were able to identify spectral positions, where the extinction coefficient is widely invariant with nanosheet size. For MoS_2, the extinction coefficient at 345 nm ($\varepsilon_{345nm}(MoS_2)$ = 68 $Lg^{-1}cm^{-1}$) can be used as universal coefficient to determine dispersed concentration over a wide size range and for WS_2, the extinction coefficient at 235 nm ($\varepsilon_{235nm}(WS_2)$ = 48 $Lg^{-1}cm^{-1}$) is widely size invariant.

In addition to length effects, the extinction spectra also contain information on mean nanosheet thickness. These result in shifts of the A-exciton position (**Figure 3H**) towards lower wavelengths as the nanosheet thickness is reduced. We determine the center of mass peak position of the A-exciton from the second derivatives to link changes in the spectral profile quantitatively to mean nanosheet thickness according to equations 5 and 6. Both MoS_2 and WS_2 follow a logarithmical relation with the same slope. We attribute these shifts to changes in the band structure with layer number and changes in the average dielectric constant around the TMD units with layer number.

The protocol describes the state-of-the-art liquid exfoliation of layered materials and their size selection by liquid cascade centrifugation. MoS_2 and WS_2 in aqueous surfactant solution are chosen as model systems. However, it can be applied to other layered materials or solvent systems. This versatility is a great strength, as it makes a broad range of materials with reasonably well-defined size available in liquids. In addition, a detailed description on the accurate lateral size and thickness determination using statistical microscopy is provided. Even though microscopy is widely used as an analysis tool, extreme care must be taken to obtain accurate and reliable statistics, as inadequate sample preparation (such as depositing high concentration samples) and inaccurate analysis and imaging can dramatically bias the statistical mean values.

Even though extremely important, this statistical microscopy is at the same time a bottle-neck in making high quality samples of liquid exfoliated nanomaterials accessible. This is simply because the procedure is tedious and time-consuming. In this manuscript, we also discuss an alternative to circumvent this problem. The principle is based on relating nanosheet sizes and thicknesses quantitatively to their optical spectra such as extinction spectra. These vary significantly and systematically as a function of size. This can be used to extract quantitative information on both nanosheet lateral size and thickness from the optical spectra. Such metrics are extremely powerful, as, once calibrated, they provide the nanosheet size and thickness information within minutes. The advantage of this is at least two-fold. On the one hand, they can be used to improve and understand both exfoliation and size selection by other techniques than the ones applied here. On the other hand, they offer the unique opportunity to produce samples with known size and thickness easily to enable the study of size effects both for fundamental studies and applications. In addition, it should be noted that the similarities between the MoS_2 and WS_2 metrics are highly encouraging and suggest that — with this protocol at hand — similar metrics can be established for other layered materials.

Disclosures

The authors have nothing to disclose.

Acknowledgements

The research leading to these results has received funding from the European Union Seventh Framework Program under grant agreement n °604391 Graphene Flagship. C.B. acknowledges the German Research Foundation, DFG, under grant BA 4856/2-1.

References

1. Zhang, H. Ultrathin Two-Dimensional Nanomaterials. *ACS Nano.* **9**, 9451-9469 (2015).
2. Yi, M., & Shen, Z. A review on mechanical exfoliation for the scalable production of graphene. *J. Mat. Chem. A.* **3**, 11700-11715 (2015).
3. Jariwala, D., Sangwan, V. K., Lauhon, L. J., Marks, T. J., & Hersam, M. C. Emerging Device Applications for Semiconducting Two-Dimensional Transition Metal Dichalcogenides. *ACS Nano.* **8**, 1102-1120 (2014).
4. Nicolosi, V., Chhowalla, M., Kanatzidis, M. G., Strano, M. S., & Coleman, J. N. Liquid Exfoliation of Layered Materials. *Science.* **340**, 1420 (2013).
5. Butler, S. Z., *et al.* Progress, Challenges, and Opportunities in Two-Dimensional Materials Beyond Graphene. *ACS Nano.* **7**, 2898-2926 (2013).
6. Bonaccorso, F., Bartolotta, A., Coleman, J. N., & Backes, C. Two-dimensional crystals-based functional inks. *Adv. Mater.*, accepted (2016).
7. Torrisi, F., & Coleman, J. N. Electrifying inks with 2D materials. *Nat. Nanotechnol.* **9**, 738-739 (2014).
8. Coleman, J. N., *et al.* Two-Dimensional Nanosheets Produced by Liquid Exfoliation of Layered Materials. *Science.* **331**, 568-571 (2011).
9. Smith, R. J., *et al.* Large-Scale Exfoliation of Inorganic Layered Compounds in Aqueous Surfactant Solutions. *Adv. Mater.* **23**, 3944-3948 (2011).
10. Khan, U., O'Neill, A., Porwal, H., May, P., Nawaz, K., & Coleman, J. N. Size selection of dispersed, exfoliated graphene flakes by controlled centrifugation. *Carbon.* **50**, 470-475 (2012).
11. Kang, J., Seo, J.-W. T., Alducin, D., Ponce, A., Yacaman, M. J., & Hersam, M. C. Thickness sorting of two-dimensional transition metal dichalcogenides via copolymer-assisted density gradient ultracentrifugation. *Nat. Commun.* **5**, 5478 (2014).
12. Backes, C., *et al.* Edge and Confinement Effects Allow in situ Measurement of Size and Thickness of Liquid-Exfoliated Nanosheets. *Nat. Commun.* **5**, 4576 ncomms5576 (2014).
13. Backes, C., *et al.* Production of Highly Monolayer Enriched Dispersions of Liquid-Exfoliated Nanosheets by Liquid Cascade Centrifugation. *ACS Nano.* **10** 1589-1601 (2016).
14. Green, A. A., & Hersam, M. C. Solution Phase Production of Graphene with Controlled Thickness via Density Differentiation. *Nano Lett.* **9**, 4031-4036 (2009).

15. Harvey, A., *et al.* Preparation of Gallium Sulfide Nanosheets by Liquid Exfoliation and Their Application As Hydrogen Evolution Catalysts. *Chem. Mater.* **27**, 3483-3493 (2015).
16. Hanlon, D., *et al.* Liquid Exfoliation of Solvent-Stabilised Few-Layer Black Phosphorus for Applications Beyond Electronics. *Nat. Commun.* **6**, 8563 ncomms9563 (2015).
17. Backes, C., *et al.* Spectroscopic metrics allow in-situ measurement of mean size and thickness of liquid-exfoliated few-layered graphene nanosheets. *Nanoscale.* **8**, 4311-4323 (2016).
18. Rodenburg, J. *Tutorial Courses on Transmission Electron Microscopy.*, <http://www.rodenburg.org/> (2016).
19. Ridings, C., Warr, G. G., & Andersson, G. G. Composition of the outermost layer and concentration depth profiles of ammonium nitrate ionic liquid surfaces. *Phys. Chem. Chem. Phys.* **14**, 16088-16095 (2012).
20. Nemes-Incze, P., Osváth, Z., Kamarás, K., & Biró, L. P. Anomalies in thickness measurements of graphene and few layer graphite crystals by tapping mode atomic force microscopy. *Carbon.* **46**, 1435-1442 (2008).
21. Paton, K. R., *et al.* Scalable production of large quantities of defect-free few-layer graphene by shear exfoliation in liquids. *Nat. Mater.* **13**, 624-630 (2014).
22. Novoselov, K. S., *et al.* Two-dimensional atomic crystals. *Proc. Nat. Ac. Sci. U. S.* **102**, 10451-10453 (2005).
23. Kouroupis-Agalou, K., *et al. Nanoscale.* **6**, 5926-5933 (2014).
24. Hanlon, D., *et al.* Production of Molybdenum Trioxide Nanosheets by Liquid Exfoliation and Their Application in High-Performance Supercapacitors. *Chem. Mater.* **26**, 1751-1763 (2014).
25. Yadgarov, L., *et al.* Dependence of the Absorption and Optical Surface Plasmon Scattering of MoS2 Nanoparticles on Aspect Ratio, Size, and Media. *ACS Nano.* **8**, 3575-3583 (2014).
26. Wilson, J. A., & Yoffe, A. D. Transition metal dichalcogenides. Discussion and interpretation of the observed optical, electrical, and structural properties. *Adv. Phys,.* **18**, 193-335 (1969).

